

Ionospheric turbulence from TEC variations and VLF/LF transmitter signal observations before and during the destructive seismic activity of August and October 2016 in Central Italy

Contadakis M.E.⁽¹⁾, Arabelos D.N.⁽¹⁾, Vergos G.S.⁽¹⁾, Skeberis Ch.⁽²⁾, Xenos T.D.⁽²⁾, Biagi P.F.⁽³⁾, Scordilis, E.M.⁽⁴⁾

⁽¹⁾ Department of Geodesy and Surveying, Aristotle University of Thessaloniki, Greece

⁽²⁾ Department of Electrical & Computer Engineering, Aristotle University of Thessaloniki, Thessaloniki, Greece

⁽³⁾ Department of Physics, University of Bari, Bari, Italy

⁽⁴⁾ Department of Geophysics, Aristotle University of Thessaloniki, Greece

Abstract. In this paper we investigate the ionospheric turbulence from observations of TEC variations as well as from VLF/LF transmitter signal observations before and during the disastrous seismic activity of August and October 2016 in Central Italy. The results of this investigation indicate that the High-Frequency limit f_o , of the ionospheric turbulence content, increases as the site and the moment of the earthquake occurrence is approaching, pointing to the earthquake locus.

Key words Seismicity, Ionospheric turbulence, VLF/LF transmission, Brownian walk, HHT

1. Introduction

It is argued that tectonic activity during the earthquake preparation period produces anomalies at the ground level which propagate upwards in the troposphere as Acoustic or Standing gravity waves (Hayakawa et al. 2011, Hayakawa 2011). These Acoustic or Gravity waves affect the turbidity of the lower ionosphere, where sporadic Es-layers may appear too, and the turbidity of the F layer. Subsequently the produced disturbance starts to propagate in the ionosphere's waveguide as gravity wave. The inherent frequencies of the acoustic or gravity wave range between 0.003Hz (period 5min) and 0.0002Hz (period 100min), which according to Molchanov et al. (2004, 2006) correspond to the frequencies of the turbulent produced by tectonic activity during the earthquake preparation period. During this propagation the higher frequencies are progressively dumped. Thus observing the frequency content of the ionospheric turbidity we will observe a decrease of the higher limit of the turbidity frequency band.

In this paper we investigate the ionospheric turbulence from the observations of TEC variations as well as from VLF/LF transmitter signal observations before and during the disastrous seismic activity of August and October 2016 in Central Italy. The Total Electron Content (TEC) data of 8 Global Positioning System (GPS) stations of the EUREF network, which are being provided by IONOLAB (Turkey), were analysed using Discrete Fourier Analysis in order to investigate the TEC variations (Contadakis et al. 2009; Contadakis et al. 2012; Contadakis et al. 2015). The data acquired for VLF/LF signal observations are from the receiver of Thessaloniki (40.59N, 22.78E), Greece (Skeberis et al. 2015) which monitor the VLF/LF transmitters of the International

Network for Frontier Research on Earthquake Precursors (INFREP). A method of normalization according to the distance between the receiver and the transmitter is applied on the above data and then they are processed by the Hilbert Huang Transform (HHT) to produce the corresponding spectra for visual analysis.

2. Seismotectonic Information of Central Italy

A series of strong earthquakes struck central Italy within a two months period during 2016, causing human losses and extensive damage in constructions. The excited area is located close to the center of the Apennines mountain belt, a well-known seismically active formation that extends in a NW-SE direction. This seismically active zone was formed during Miocene-Pliocene due to the subduction of Adriatic microplate beneath Eurasia (Italian peninsula) (e.g. Selvaggi and Amato, 1992; Amato et al., 1993; Sparkman et al., 1993; Scandone 1996 among many others). Later, during Quaternary, the stress regime turn to extensional striking in an almost ENE-WSW direction and developing a series of normal faults along the Apennines mountain belt (e.g. Patacca et al., 1990; Kruse and Royden, 1994; Cinque et al., 1993, D'Agostino et al., 2001). This chain of normal faults is responsible for the generation of the recent strong earthquakes of August and October of 2016 (24 August, $M=6.2$; 26 October, $M=6.1$; 30 October, $M=6.6$) that occurred close to the center of Apennines belt.

The map of figure (1) gives a picture of the seismicity of the Central Apennine belt where the recent activity took place. In this map are plotted the epicenters of all known earthquakes with $M \geq 3.0$ which occurred since 1900. Black ellipse delimits the seismogenic region of the Amatrice seismic sequence with its three strong ($M > 6.0$) shocks. In the same map are shown the epicenters of other three strong events that occurred in the broader area since the beginning of the 20th century (see table 1). The focal parameters are mainly adopted from the on-line earthquake catalog of the International Seismological Centre (ISC, <http://www.isc.ac.uk>). All magnitudes are given in the moment magnitude scale, M_w , and are either adopted (when original estimations were available) or estimated by applying proper relations converting other magnitude scales to M_w (Scordilis 2006; Tsampas, 2006; Duni et al., 2010).

The Amatrice seismic sequence was generated on a NW-SE oriented (and dipping to the SW) system of normal faults. According to GCMT (Global Centroid Moment Tensor project, <http://www.globalcmt.org>) the activated segment that gave the strongest earthquake of the sequence (October 30, 06:40, $M=6.6$) strikes in $N149^\circ$ direction and dips to the SW at an angle of 38° . The seismogenic region that is formed by the epicenters of the aftershocks (see figure 1) delineates a presumable fault zone of a length of ~ 30 km, justifying the generation of a characteristic earthquake of magnitude $M \sim 6.6$ (according to Papazachos et al., 2004).

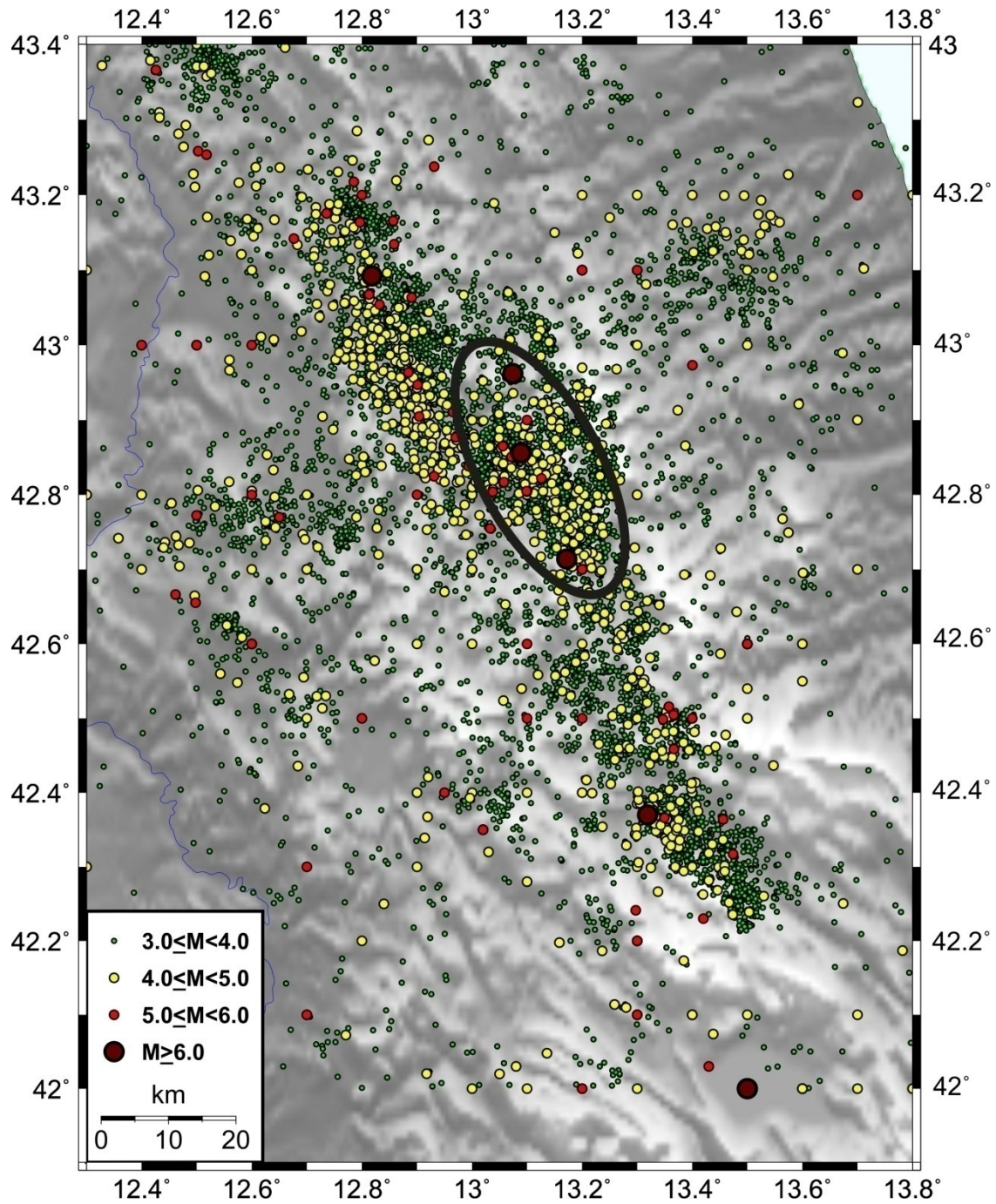


Figure 1. Epicenters of all known earthquakes with $M \geq 3.0$ that occurred during the period 1900-2016 (October) in the broader area of central-northern Apennines. The black ellipse delimits the seismogenic region of the recent(August-October 2016) Amatrice sequence.

Table 1. Focal parameters of the six strongest earthquakes than occurred close to the seismogenic region of the Amatrice sequence since 1900.

Year	Month	Day	Or. Time	Lat ($^{\circ}$ N)	Lon ($^{\circ}$ E)	M_w
1915	January	13	06:52	42.00	13.50	7.0
1997	September	26	09:40	43.09	12.82	6.0
2009	April	6	01:32	42.37	13.32	6.3
2016	August	24	01:36	42.71	13.17	6.2
2016	October	26	19:18	42.96	13.07	6.1
2016	October	30	06:40	42.86	13.09	6.6

4. TEC variation over mid latitude Europe

In the following we investigate the variations of TEC over the broader area of central Italy before and during the seismic activity of of August and October ,2016. To this purpose we use the TEC estimates provided by IONOLAB (<http://www.ionolab.org>) (Arikan et al. 2009) for 8 mid latitude GPS stations of EUREF which cover epicentre distances from the active area ranging from 382km to 2285km for the time periods between 24/07/2016 to 25/09/2016 and 25/10/ 2016 to 25/11/2016. The selected GPS stations have about the same latitude and are expected to be affected equally from the Equatorial Anomaly as well as from the Auroral storms. Table 2 displays the 8 EUREF stations while Figure 4 displays the locus of the eight GPS stations and the main shock. The IONOLAB TEC estimation system uses a single station receiver bias estimation algorithm, IONOLAB-BIAS, to obtain daily and monthly averages of receiver bias and is successfully applied to both quiet and disturbed days of the ionosphere for station position at any latitude. In addition, TEC estimations with high resolution are also possible (Arikan et al. 2009). IONOLAB system provides comparison graphs of its TEC estimations with the estimations of the other TEC providers of IGS in its site. In this work only TEC estimations in perfect accordance among all providers were used. The TEC values are given in the form of a Time Series with a sampling gap (resolution) of 2.5 minutes. Figures 2 and 3 display the TEC variation over the 8 EUREF stations for the time periods between 24/07/2016 to 25/09/2016 and 25/10/ 2016 to 25/11/2016, respectively.

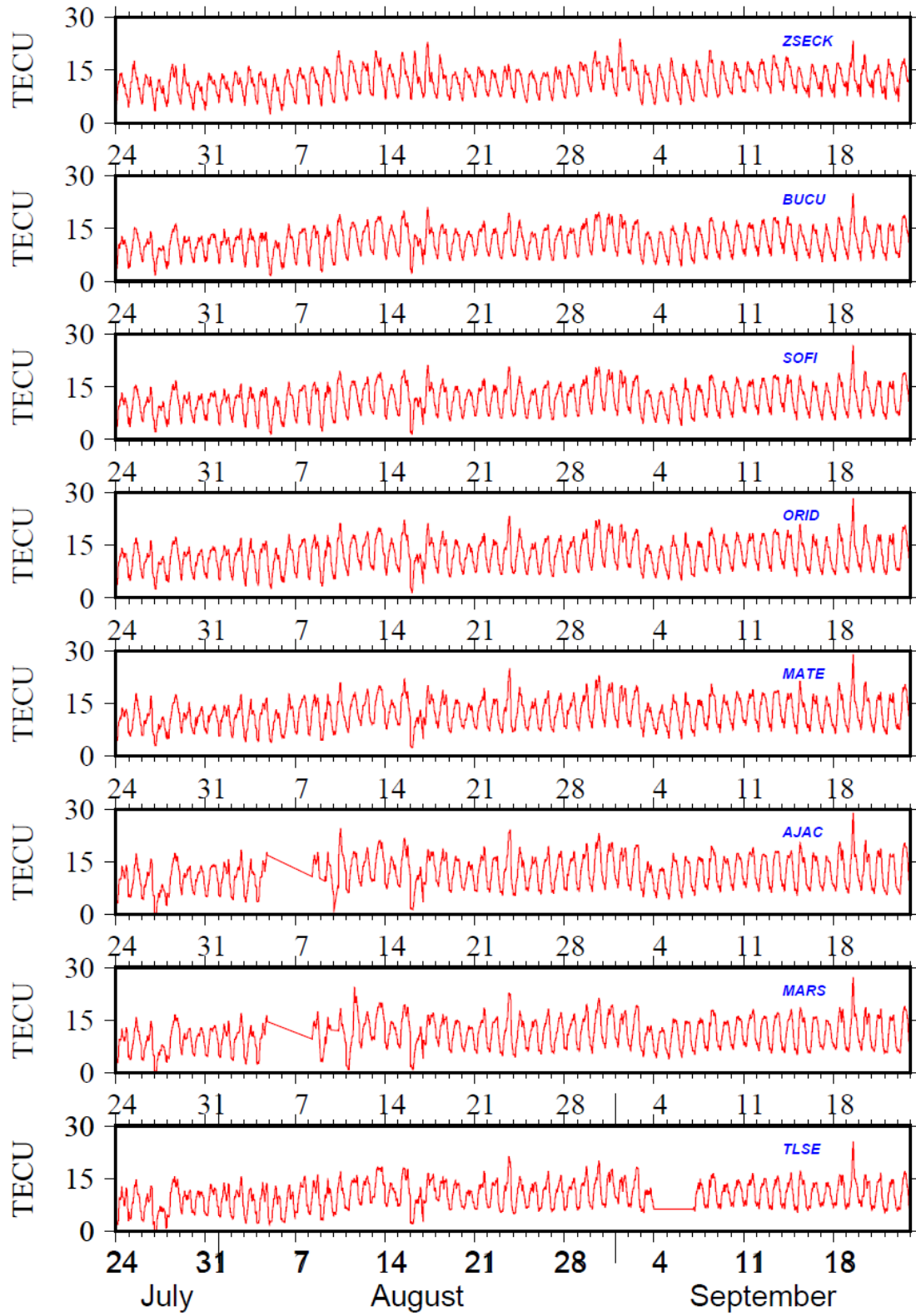


Figure 2. The variations of TEC over the 8 EUREF stations during the time period of 24/07/2016 to 25/09/2016

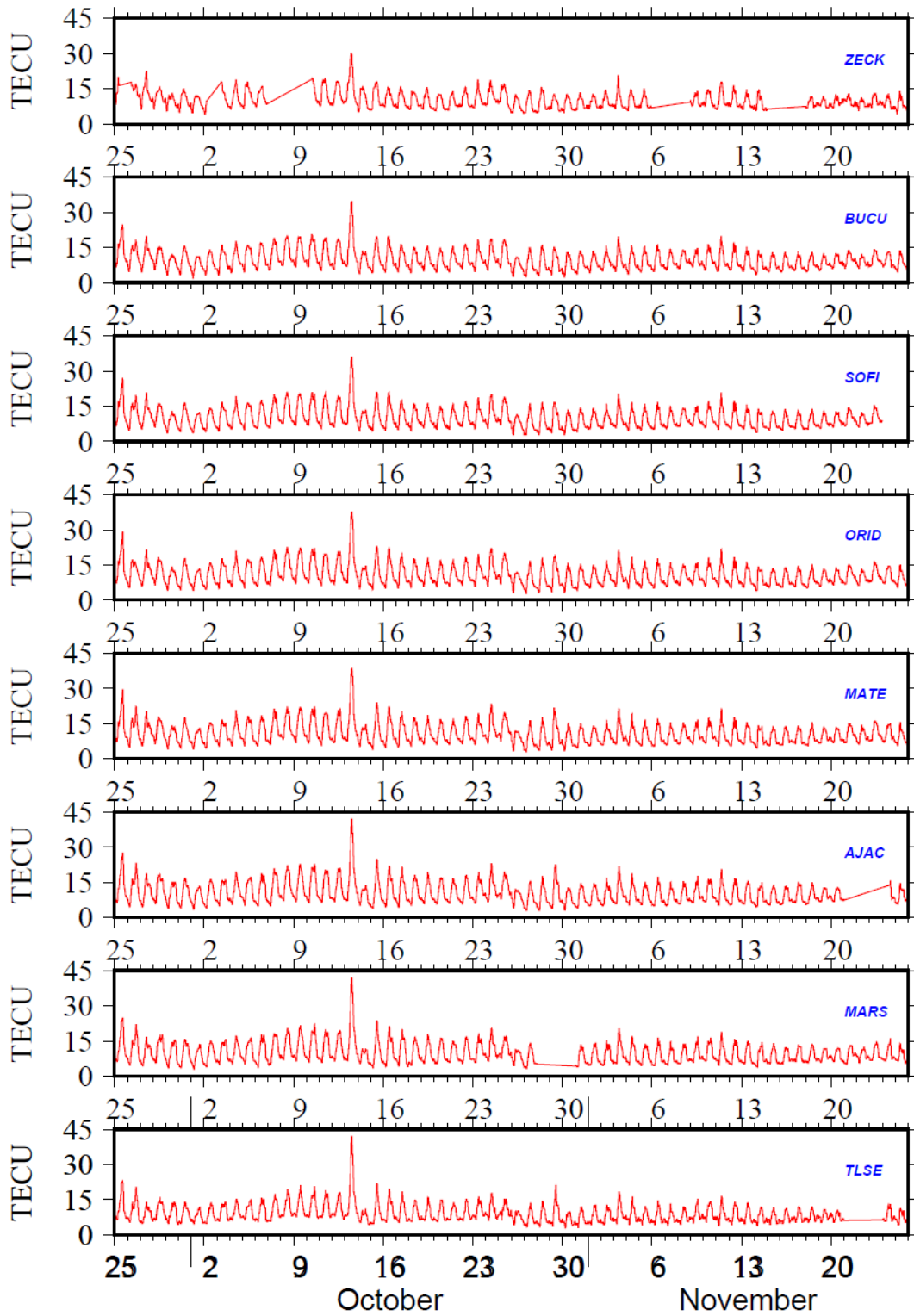


Figure 3. The variations of TEC over the 8 EUREF stations during the time period of 25/10/2016 to 25/11/2016

Table 2. Distance of GPS stations from the epicenter of the earthquake

GPS Site	Latitude Degree	Longitude Degree	Distance km
Amatrice	42.611679	13.289436	0.0
Toulouse	43.609253	1.444428	967.1
Marseille	43.299892	5.370561	648.7
Ajaccio	41.919228	8.738636	382.3
Matera	40.667267	16.604712	350.2
Ohrid	41.123657	20.801771	643.4
Sofia	42.699718	23.322260	820.0
Bucharest	44.430111	26.103037	1051.6
Zelenchukskaya	43.857071	41.585293	2285.3

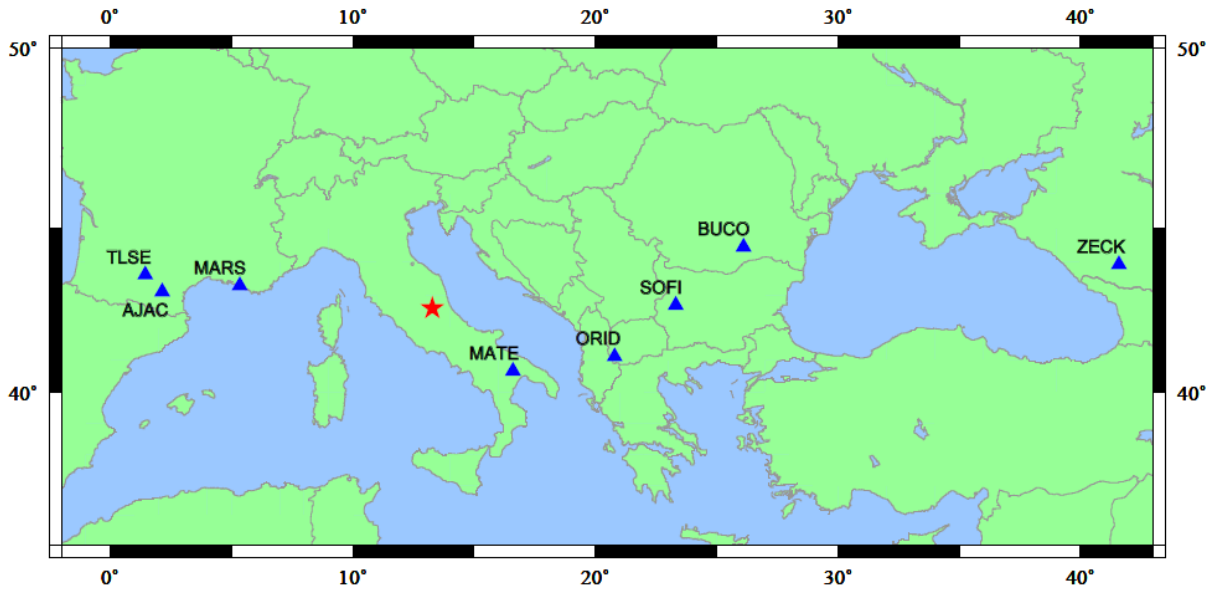


Figure 4. The locus of the GPS stations of the network (in blue) and the locus of the earthquakes of August and October, 2016 (in red)

4.1 Geomagnetic and Solar activity indices

The variations of the geomagnetic field were followed by the Dst- index and the planetary kp three hour indices quoted from the site of the Space Magnetism Faculty of Science, Kyoto University (<http://swdcwww.kugi.kyoto-u.ac.jp/index.html>) for the time period of our data. Figures 5 and 6 displays the Dst-index variations on August and October of 2016, respectively.

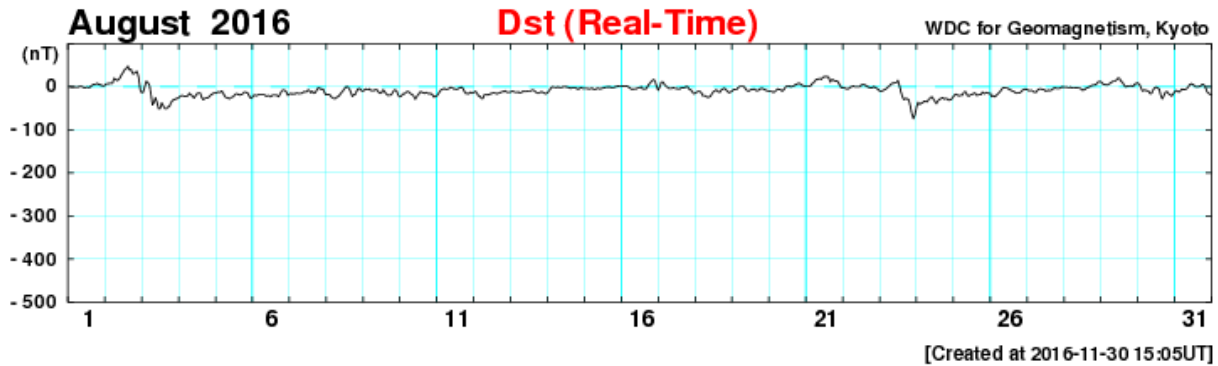


Figure 5 Dst-index variations on August of 2016

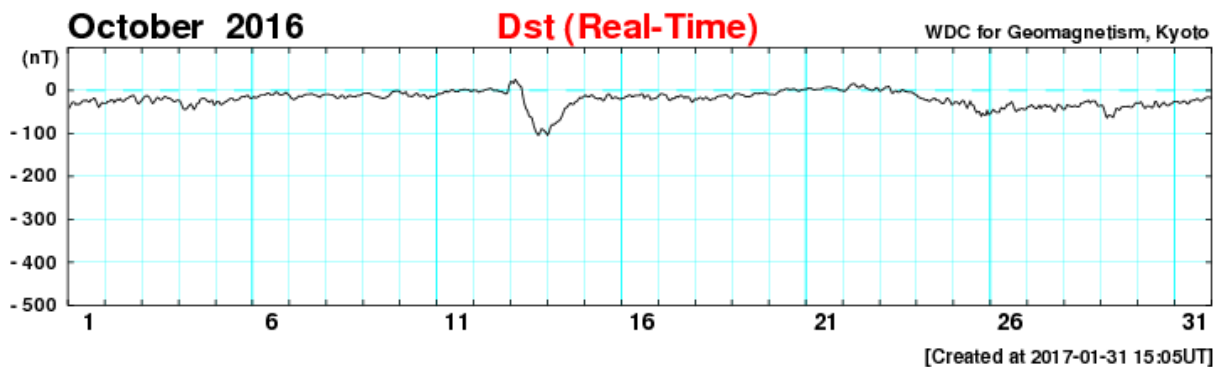


Figure 6 Dst-index variations on October of 2016

4.2 Fast Fourier Transform Analysis

The Power Spectrum of TEC variations will provide information on the frequency content of them. Apart of the well known and well expressed tidal variations, for which the reliability of their identification can be easily inferred by statistical tests, small amplitude space-temporal transient variations cannot have any reliable identification by means of a statistical test. Nevertheless looking at the logarithmic power spectrum we can recognize from the slop of the diagram whether the contributed variations to the spectrum are random or periodical. If they are random the slop will be 0, which correspond to the white noise, or -2 which correspond to the Brownian walk, otherwise the slop will be different the so called Fractal Brownian walk (Turcotte, 1997). This means that we can trace the presence of periodical variations in the logarithmic power spectrum of TEC variations.

This method was successfully applied in our previous work (Contadakis et al. 2008, Contadakis et al. 2012, Contadakis et al. 2015) in order to find the frequency content of TEC turbidity. It is realized that the upper frequency limit f_0 of the spectrum of TEC variations increases as we approach the source of the ionospheric turbidity modulation, in our case the earthquake preparation activity.

4.3 Results

Figures 7 and 8 display the variation of TEC turbulence frequency limit f_o over the the selected EUREF GPS stations for the shock of 24 August and the same show Figures 9 and 10 for the shocks of 26/30 October, 2016. All graphs indicate time and space convergence of increasing turbulence frequency limit f_o to the earthquakes of 24 August and 26/30 October, occurrence. Hobarat et al.(2005) in a study on the ionospheric turbulence in Low latitudes concluded that the attribution of the turbulence to earthquake process and not to other sources, i.e. solar activity, storms etc is not conclusive. Never the less in our case, the steady monotonic, time and space, convergence of the frequency limit f_o increment, to the occurrence of the Amatrice earthquakes of 24/08 and 26&30/ 10 is a strong decisive indication that the observed turbidity is generated by the respective earthquakes preparation processes.

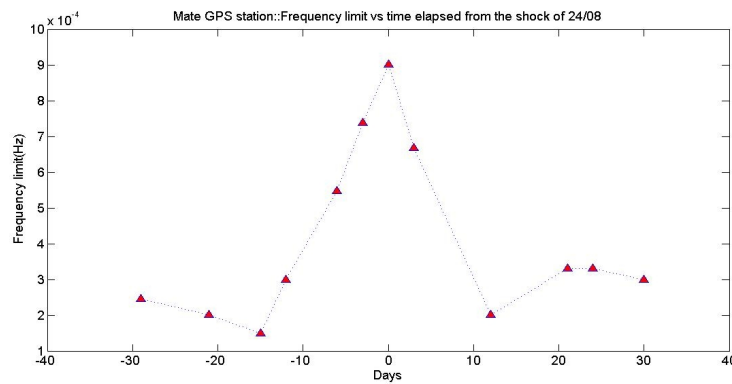


Figure 7. Variation of TEC turbulence frequency limit f_o over the closest to Amatrice GPS Stations of Matera, with the time distance from the day of the earthquake of 24 August, 2016 occurrence

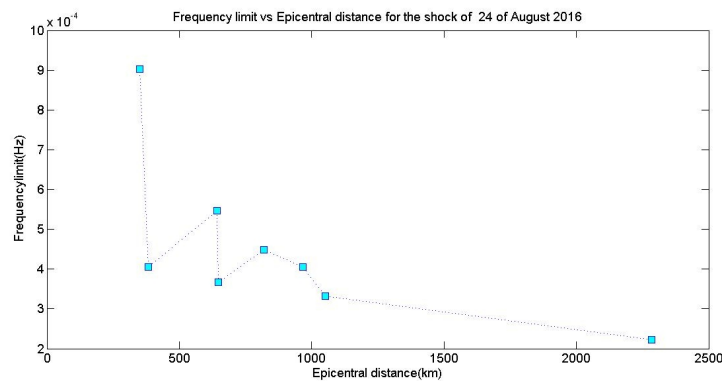


Figure 8. Variation of TEC turbulence frequency limit f_o over the GPS Stations of EUREF, with the epicentral distance around the day of the earthquake of 24 August, 2016 occurrence.

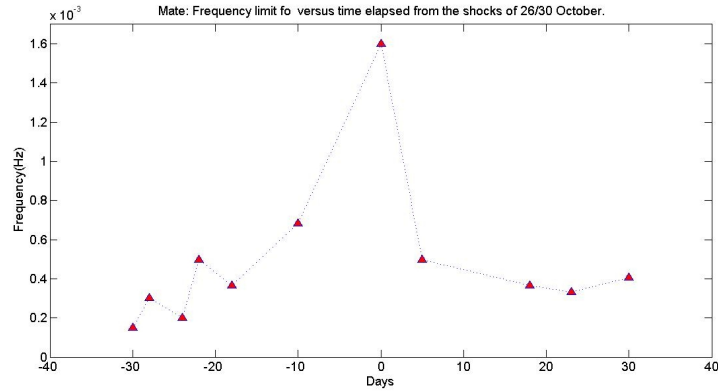


Figure 9. Variation of TEC turbulence frequency limit f_o over the closest to Amatrice GPS Stations of Matera, with the time distance from the day of the earthquake of 26/30 October, 2016 occurrence

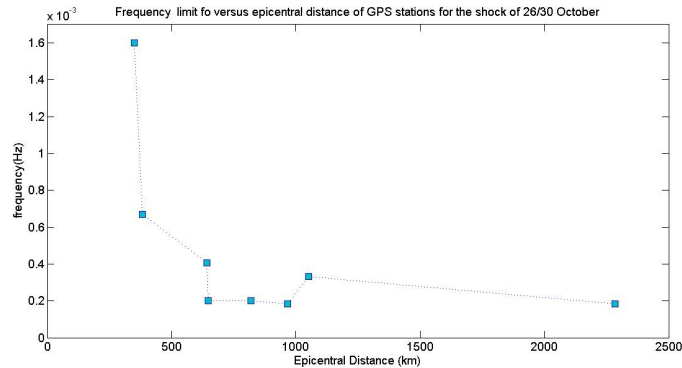


Figure 10. Variation of TEC turbulence frequency limit f_o over the GPS Stations of EUREF, with the epicentral distance around the day of the earthquake of 26/30 October, 2016 occurrence.

The qualitative explanation of this phenomenology can be offered on the basis of the LAIC: Tectonic activity during the earthquake preparation period produces anomalies at the ground level which propagate upwards in the troposphere as Acoustic or Standing gravity waves (Hayakawa et al. 2011, Hayakawa 2011). These Acoustic or Gravity waves affect the turbidity of the lower ionosphere, where sporadic Es-layers may appear too, and the turbidity of the F layer. Subsequently the produced disturbance starts to propagate in the ionosphere's waveguide as gravity wave and the inherent frequencies of the acoustic or gravity wave can be traced on TEC variations (i.e. the frequencies between 0.003Hz (period 5min) and 0.0002Hz (period 100min), which according to Molchanov et al. (2004, 2006) correspond to the frequencies of the turbulent induced by the LAIC coupling process to the ionosphere. As we move far from the disturbed point, in time or in space, the higher frequencies (shorter wavelength) variation are progressively attenuated

5. Detection of VLF/LF disturbances.

In the frame of the International Network for Frontier Research on Earthquake Precursors (INFREP) (Biagi et al. 2011) a receiver in Thessaloniki, Greece (40.59N, 22.78E) is monitoring the VLF transmitters based in Tavolara, Italy, Niscemi, Italy, and Le Blanc, France. (Skeberis et al. 2015). The transmission paths of these transmitters to the Thessaloniki receiver passes over the broader area of the Amatrice earthquakes epicenters. Figure 11 displays the transmitters of the INFREP Network which are monitored by the receiver of Thessaloniki and Table 3 displays the sites and the transmitting frequencies of these transmitters.

Table 3. The Transmitters of the INFREP Network which are monitored by the Thessaloniki receiver

Freq. (KHz)	Station	Location	Lat/Lon
19.58	GBZ	Anthorn, UK	54° 54' 40'' N 03° 16' 48'' W
20.27	ICV	Tavolara, IT	40° 54' 22'' N 09° 42' 48'' E
23.4	HWU	Le Blanc, FR	53° 04' 57'' N 07° 36' 55'' E
37.5	ICE	Keflavik, IS	64° 01' 00'' N 22° 34' 00'' W
45.9	NSY	Niscemi, IT	37° 07' 32'' N 14° 26' 11'' E
153	ROM	Brasov, RO	45° 45' 17'' N 25° 36' 24'' E
180	TRT	Polalti, TR	39° 45' 22'' N 43° 25' 05'' E
183	EU1	Felsberg, DE	49° 16' 49'' N 06° 40' 41'' E
198	CN1	Berkaoui, DZ	31° 55' 14'' N 05° 04' 03'' E
270	CZE	Topolna, CZ	49° 07' 25'' N 17° 30' 52'' E

5.1 Data Analysis

The data are processed by the Hilbert Huang Transform (HHT) (Skeberis et al. 2015) which is a two step process. The first step of the process is the Complete Ensemble Empirical Mode Decomposition with Adaptive Noise (CEEMDAN) which devolves the signal to its Intrinsic Mode Functions (IMFs) and the second step of the process is a Hilbert Transform on the IMFs and subsequent production of the relevant spectra (Hilbert Amplitude Spectrum). In the produced spectra by selecting appropriately wide time windows we can easily discern periods of calm and more importantly we can pinpoint areas which are of interest and can denote disturbances in the signals received during their propagation through the ionosphere. By eliminating other sources like geomagnetic storms (by going through the relevant geomagnetic indices of Ap and Kp) we can safely assume that the disturbances cause can be mainly attributed to the ionosphere, and are related to the seismic phenomenon in question.



Figure 11. The INFREP Network. Whit star indicate Amatrice earthquakes epicenter

During calm periods of no appreciable activity we can easily discern a normal pattern that is characterized by a diurnal fluctuation during the night and day cycles and no exceptional peaks that can be characterized as disturbances. In the days prior to the earthquake, precursors can be

seen as peaks that are breaking the pattern of normal fluctuations, with easily detectable peaks especially located in the higher frequency regions of the produced spectra. In those peaks we can detect an anomalous behaviour in the waveguide between transmitter and receiver that can be attributed to precursor phenomena prior to the occurrence of the earthquake.

5.2 Results

In the instance of the chain of earthquakes that occurred in Italy in August 2016, culminating in the earthquake on 24th of August 2016 ($M_w=6.2$) and in October 2016, culminating in the earthquake on 26th of October 2016 ($M_w=6.1$) and the earthquake on 30th of October 2016 ($M_w=6.5$) Figures 12 to 23 present the relevant spectra for the signals received in Thessaloniki from Tavolara on overlapping intervals (Fig. 12 for 01-08-2016 to 19-09-2016, Fig.13 for 15-08-16 to 02-09-2016, Fig.14 for 15-10-2016 to 25-10-2016 and Fig 15 for 20-10-2016 to 03-11-2016) and the same intervals for the signals received from Niscemi, Fig.16, Fig. 17, Fig.18, Fig. 19 and LeBlanc Fig. 20, Fig. 21, Fig. 22, Fig. 23.

In these spectra we can clearly see disturbances 2 to 14 days prior to the seismic events that occurred in August and October 2016 in Italy. These disturbances are turbulent in the frequency band 0.001Hz (16,7min) to 0.01Hz.(1.6min).

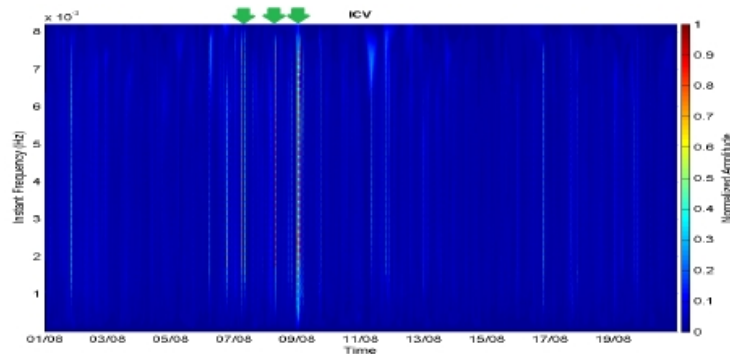


Figure 12: The spectrum of the signals received from Tavolara, Italy (ICV) - 01-08-2016 to 19-08-2016. Green arrow denotes the disturbances

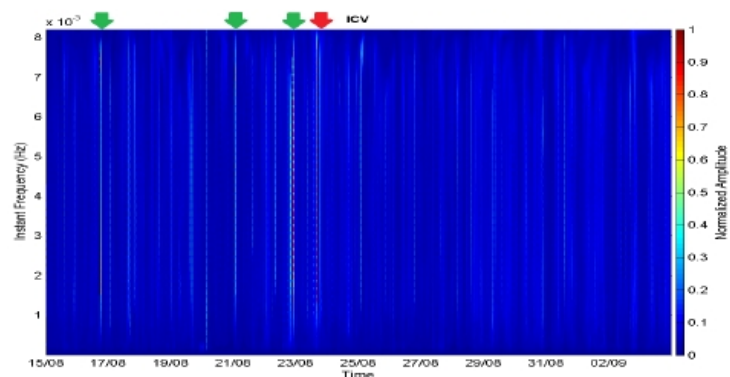


Figure. 13: The spectrum of the signals received from Tavolara, Italy (ICV) - 15-08-2016 to 02-09-2016. Green arrow denotes the disturbances - Red arrow denotes the occurrence of the earthquakes

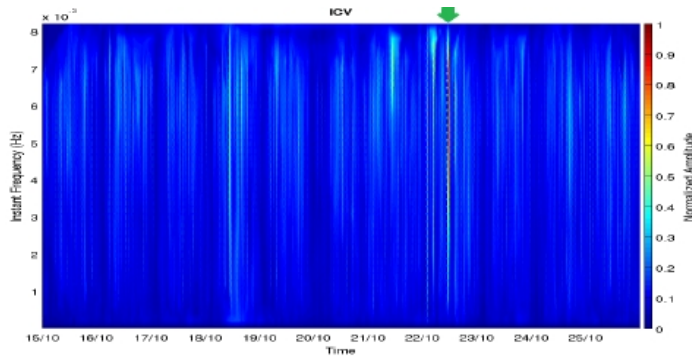


Figure 14: The spectrum of the signals received from Tavolara, Italy (ICV) - 15-10-2016 to 25-10-2016. Green arrow denotes the disturbances

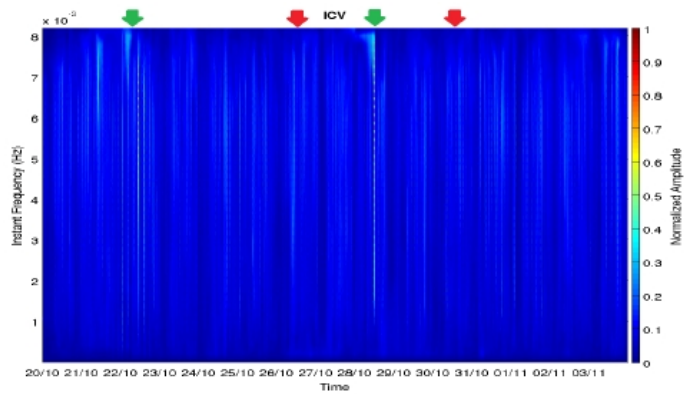


Figure15: The spectrum of the signals received from Tavolara, Italy (ICV) - 20-10-2016 to 03-11-2016. Green arrow denotes the disturbances - Red arrow denotes the occurrence of the earthquakes

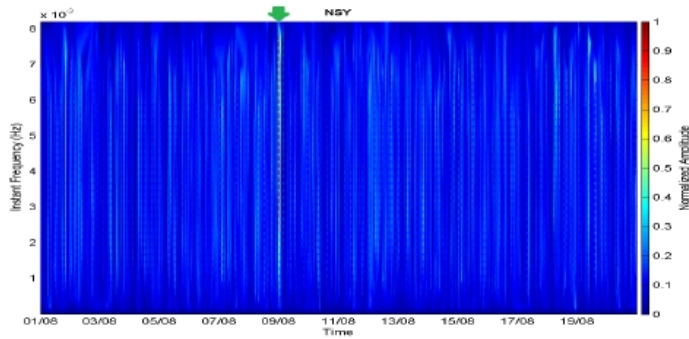


Figure 16: The spectrum of the signals received from Niscemi, Italy (NSY) - 01-08-2016 to 19-08-2016. Green arrow denotes the disturbances

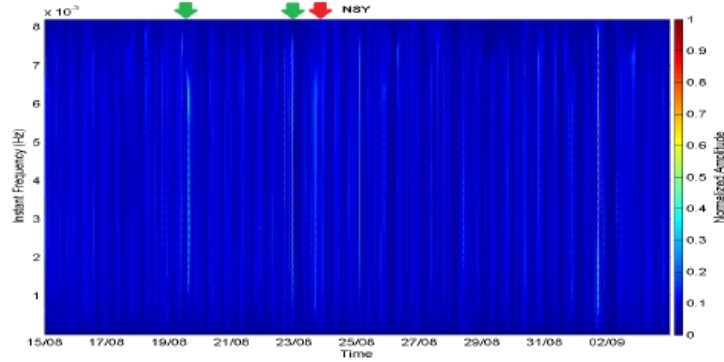


Figure 17: The spectrum of the signals received from Niscemi, Italy (NSY) - 15-08-2016 to 02-09-2016. Green arrow denotes the disturbances - Red arrow denotes the occurrence of the earthquakes

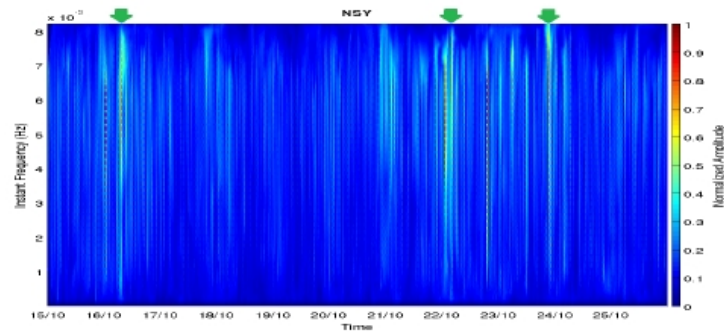


Figure 18 : The spectrum of the signals received from Niscemi, Italy (NSY) - 15-10-2016 to 25-10-2016. Green arrow denotes the disturbances

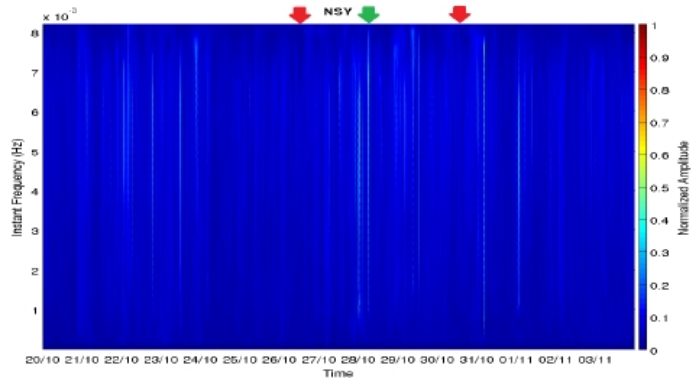


Figure 19: The spectrum of the signals received from Niscemi, Italy (NSY) - 20-10-2016 to 03-11-2016. Green arrow denotes the disturbances - Red arrow denotes the occurrence of the earthquakes

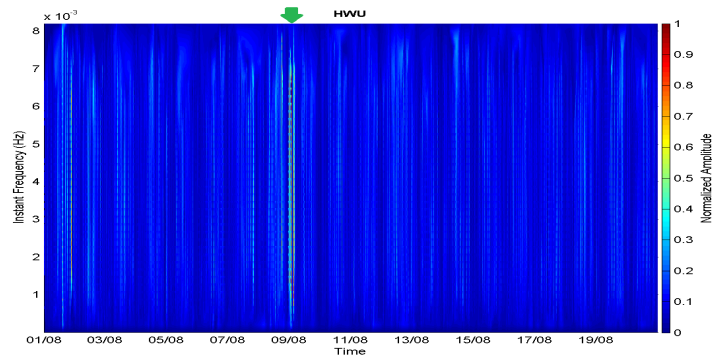


Figure 20: The spectrum of the signals received from LeBlanc, France(HWU) - 01-08-2016 to 19-08-2016. Green arrow denotes the disturbances

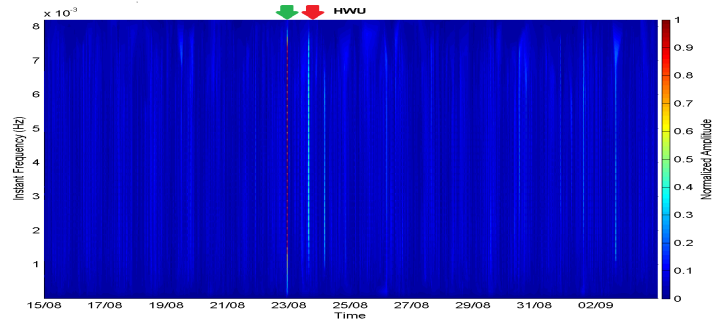


Figure 21: The spectrum of the signals received from LeBlanc, France (HWU) - 15-08-2016 to 02-09-2016. Green arrow denotes the disturbances - Red arrow denotes the occurrence of the earthquakes

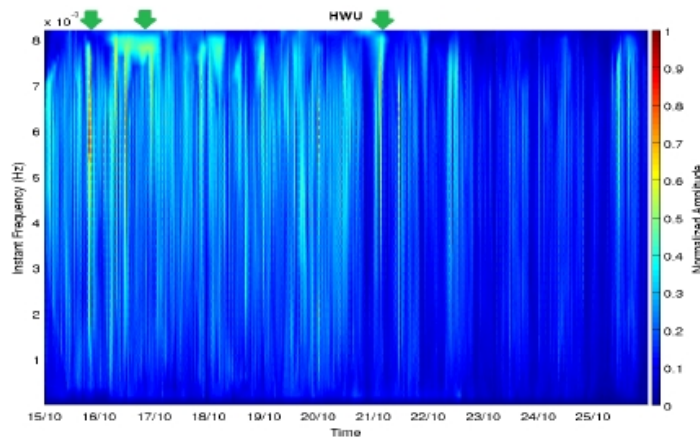


Figure 22: The spectrum of the signals received from LeBlanc, France (HWU) - 15-10-2016 to 25-10-2016. Green arrow denotes the disturbances

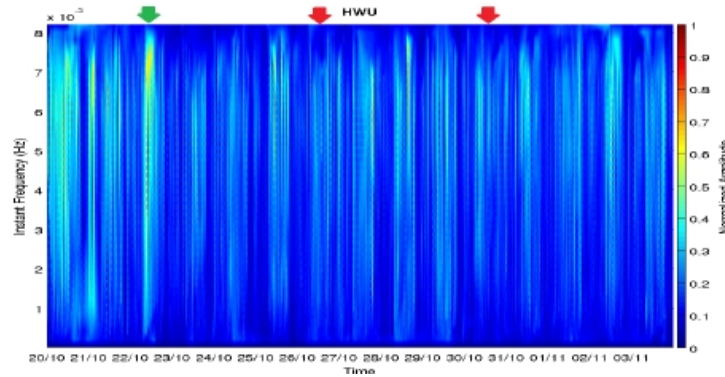


Figure 23: The spectrum of the signals received from LeBlanc, France (HWU) - 20-10-2016 to 03-11-2016. Green arrow denotes the disturbances - Red arrow denotes the occurrence of the earthquakes

6. Concluding Remark

It is shown that the frequency content of the ionospheric turbulence over the earthquake epicenter, deduced directly from GPS TEC observations or indirectly through the VLF transmission, moves to higher frequencies over the area of the epicenter of Amatrice earthquakes the last 15 days before the main shock and ranges between 0.001Hz and 0.01Hz. This observational results are consistent with the explanation that this Ionospheric turbulence modulation is a result of the earthquake preparation process disturbances transmitted to Ionosphere by a LAIC mechanism.

References

- Amato, a., B. Alessandrini, G.B. Cimini, A. Frepoli and G. Selvaggi, 1993. Active and remnant subducted slabs beneath Italy: evidence from seismic tomography and seismicity. *Ann. Geophys.*, 36 (2), 201-214.
- D'Agostino, N., J.A. Jackson, F. Dramis and R. Funiciello, 2001. Interactions between mantle upwelling, drainage evolution and active normal faulting: an example from the central Apennines (Italy). *Geophys. J. Int.*, 147, 475-497.
- Arikan, F., Yilmaz, A., Arikan, O., Sa Yin, I. Gurun, M., Yildirim, S.A. Space Weather Activities of IONOLAB Group: TEC Mapi, *Geoph. Res. Abstr.*, Vol 11, 2009
- P. F. Biagi, T. Maggipinto, F. Righetti, D. Loiacono, L. Schiavulli, T. Ligonzo, A. Ermini, I. A. Moldovan, A. S. Moldovan, A. Buyuksarac, H. G. Silva, M. Bezzeghoud, and M. E. Contadakis, 2011, The European VLF/LF radio network to search for earthquake precursors: setting up and natural/man-made disturbances, *Nat. Hazards Earth Syst. Sci.*, 11, 333-341
- Cinque, a., A. Patacca, P. Scandone and M. Tozzi, 1993. Quaternary kinematic evolution of the Arikan, F., Yilmaz, A., Arikan, O., Sa Yin, I. Gurun, M., Yildirim, S.A. Space Weather Activities of IONOLAB Group: TEC Mapi, *Geoph. Res. Abstr.*, Vol 11, 2009
- Contadakis, M.E., Arabelos, D.N., Asteriadis, G., Spatalas, S.D., Pikridas, C. TEC variations over the Mediterranean during the seismic activity period of the last quarter of 2005 in the area of Greece, *Nat. Hazards and Earth Syst. Sci.*, 8, 1267-1276, 2008.

- Contadakis, M.E., Arabelos, D.N., Asteriadis, G., Spatalas, S.D., Pikridas, C. TEC variations over Southern Europe before and during the M6.3 Abruzzo earthquake of 6th April 2009, *Annals of Geophysics*, vol. 55, iss. 1, p. 83-93, 2012a.
- Contadakis, M. E., Arabelos, D.N., Vergos, G., Spatalas, S. D., Skordilis, M., 2015, TEC variations over the Mediterranean before and during the strong earthquake (M = 6.5) of 12th October 2013 in Crete, Greece, *Physics and Chemistry of the Earth*, Volume 85, p. 9-16
- Duni, L., Sh.Kuka and N.Kuka, 2010. Local relations for converting M_L to M_W in southern-western Balkan region. *Acta Geod. Geoph. Hung.*, 45(3), 317–323.
- Hayakawa, M. On the fluctuation spectra of seismo-electromagnetic phenomena, *Nat. Hazards Earth Syst. Sci.*, 11, 301-308, 2011.
- Hayakawa, M., Kasahara, Y., Nakamura, T., Hobara, Y., Rozhnoi, A., Solovieva, M., Molchanov, O.A. and Korepanov, V., 2011, Atmospheric gravity waves as a possible candidate for seismo-ionospheric perturbations, *J. Atmos. Electr.*, 32, 3, 129-140.
- Hobara Y., Lefeuvre F., Parrot M., and Molchanov O. A., 2005 Low-latitude ionospheric turbulence observed by Aureol-3 satellite, *Annales Geophysicae*, 23, 1259–1270
- Kruse, S. and L.H. Royden, 1994. Bending and unbending of an elastic lithosphere: the Cenozoic history of the Apennine and Dinaride foredeep basins. *Tectonics*, 13, 278-302.
- Molchanov, O., Biagi, P.F., Hayakawa, M., Lutikov, A., Yunga, S., Iudin, D., Andreevsky, S., Rozhnoi, A., Surkov, V., Chebrov, V., Gordeev, E., Schekotov, A., Fedorov, E., Lithosphere-atmosphere-ionosphere coupling as governing mechanism for preseismic short-term events in atmosphere and ionosphere, *Nat. Hazards Earth Syst. Sci.*, 4, 5/6, 757-767, 2004.
- Molchanov, O., Schekotov, A., Solovieva, M., Fedorov, E., Gladyshev, V., Gordeev, E., Chebrov, V., Saltykov, D., Sinitsin, V.I., Hattori, K., Hayakawa, M. Near seismic effects in ULF fields and seismo-acoustic emission: statistics and explanation, *Nat. Hazards Earth Syst. Sci.*, 5, 1-10, 2005
- Papazachos, B.C., E.M. Scordilis, D.G. Panagiotopoulos, C.B. Papazachos and G.F. Karakaisis, 2004. Global relations between seismic fault parameters and moment magnitude of earthquakes, *“Bulletin of the Geological Society of Greece”*, XXXVI, 3, 1482-1489.
- Patacca, E., R. Sartori and P. Scandone, 1990. Tyrrhenian basin and Apennine arcs: kinematic relations since late Tortonian times. *Mem. Soc. Geol. It.*, 45, 425-451.
- Rozhnoi A., Solovieva M., Parrot M., Hayakawa M., Biagi P.F., Schwingenschuh K., 2012, Ionospheric turbulence from ground-based and satellite VLF/LF transmitter signal observations for the Simushir earthquake (November 15, 2006), *Annals of Geophysics*, 55, 1, 2012; doi: 10.4401/ag-5190
- Scandone, P., 1996. Linea di Ricerca 2 “Sismotettonica”. In: Corsanego, A., Faccioli, E., Gavarini, C., Scandone, P., Slejko, D., Stucchi, M. (Eds.), *L'attivit  del GNNDT nel triennio 1993–1995*. CNR-GNNDT, Rome, pp. 67–96.
- Skeberis, C., Zaharis, Z. D., Xenos, T. D., Spatalas, S., Arabelos, D. N., & Contadakis, M. E. (2015). Time–frequency analysis of VLF for seismic-ionospheric precursor detection: Evaluation of Zhao-

Atlas-Marks and Hilbert-Huang Transforms. *Physics and Chemistry of the Earth, Parts A/B/C*, 85, 174-184

Schuster, A., 1897, On lunar and solar periodicities of earthquakes, *Proc. R.Soc. Lond.*, 61, 455-465

Turcotte D.L. *Fractal and Chaos in Geology and Geophysics* (2nd Edition), Cambridge University Press, Cambridge U. K., 1997.